

## Interaction of Monoheteryl Substituted Cationic Porphyrins with Synthetic Nucleic Acids

N. Sh. Lebedeva,<sup>a@</sup> E. S. Yurina,<sup>a</sup> S. S. Guseinov,<sup>a</sup> and O. I. Koifman<sup>b</sup>

<sup>a</sup>G.A. Krestov Institute of Solution Chemistry of the Russian Academy of Sciences, 153045 Ivanovo, Russia

<sup>b</sup>N.D. Zelinsky Institute of Organic Chemistry, 119991 Moscow, Russia

@Corresponding author E-mail: nsl@isc-ras.ru

*The complex formation of monoheteryl-substituted tricationic porphyrins with representative polynucleotides (poly[d(GC)2] and poly[d(AT)2]) was studied. It has been spectrally established that the studied porphyrins form intercalation complexes of different geometry with poly[d(GC)2]: 1) intercalation between the nitrogenous bases of the porphyrin macroring; 2) intercalation between the nitrogenous bases of the monoheteryl substituent. The studied porphyrins form complexes with the poly[d(AT)2] groove. The DSC method was used to analyse the temperature dependences of the specific heat capacities of solutions of the initial reagents and complexes of porphyrins with poly[d(GC)2] and poly[d(AT)2]; it was found that the proportion of structural changes in the analysed solution associated with intercalation significantly exceeds the similar value during the formation of the complex in the groove of the nucleic acid. The results obtained demonstrate a new potential opportunity to increase the selectivity of binding of ligands to nucleic acids.*

**Keywords:** Porphyrins, nucleic acids, intercalates.

## Взаимодействие моногетерилзамещенных катионных порфиринов с синтетическими нуклеиновыми кислотами

Н. Ш. Лебедева,<sup>a</sup> Е. С. Юрина,<sup>a</sup> С. С. Гусейнов,<sup>a</sup> О. И. Койфман<sup>b</sup>

<sup>a</sup>Институт химии растворов им. Г.А. Крестова РАН, 153045 Иваново, Россия

<sup>b</sup>Институт органической химии им. Н. Д. Зелинского РАН, 119991 Москва, Россия

@E-mail: nsl@isc-ras.ru

*Изучено комплексообразование моногетерилзамещенных трикатионных порфиринов с репрезентативными полинуклеотидами: poly[d(GC)2] и poly[d(AT)2]. Спектрально установлено, что исследуемые порфирины образуют с poly[d(GC)2] интеркаляционные комплексы различной геометрии: 1) с интеркаляцией между азотистыми основаниями порфиринового макрокольца; 2) с интеркаляцией между азотистыми основаниями моногетерильного заместителя. Изученные порфирины образуют комплексы с бороздкой poly[d(AT)2]. Методом ДСК при анализе температурных зависимостей удельных теплоемкостей растворов исходных реагентов и комплексов порфиринов с poly[d(GC)2] и poly[d(AT)2] установлено, что доля структурных изменений в анализируемом растворе, связанных с интеркаляцией, существенно превышает аналогичную величину при образовании комплекса в бороздке нуклеиновой кислоты. Полученные результаты демонстрируют новую потенциальную возможность повышения селективности связывания лигандов с нуклеиновыми кислотами.*

**Ключевые слова:** Порфирины, нуклеиновые кислоты, интеркаляты.

## Introduction

Cancer is characterized by the uncontrolled growth and proliferation of cells due to a genetic mutation. Cancer is one of the most important health problems and the second leading cause of death.<sup>[1]</sup> Some estimates predict 22 million new cases per year by 2030. The synthesis and evaluation of new anticancer therapeutics is critically needed to overcome the remaining shortcomings of existing drug compounds, including side effects, lower efficacy against certain cancers, and innate or acquired drug resistance.<sup>[2-4]</sup> The search for and creation of new drug candidates with antitumor activity has become one of the most important tasks for medicinal chemistry. Among the most important chemotherapeutic agents used in the treatment of cancer are those that intercalate into DNA, *i.e.* inserted between pairs of nitrogenous bases in DNA. Intercalation causes local structural changes in the DNA molecule, its elongation due to the unwinding of the double helix.<sup>[5]</sup> Intercalates are mutagenic causing slowing or even inhibition of transcription and DNA replication.<sup>[6]</sup> Porphyrin compounds are promising candidates because they can interact with DNA intercalationally or by binding in the DNA major/minor groove or form weak external complexes due to electrostatic interaction with the DNA phosphate backbone. The main advantage of porphyrins, compared with traditional intercalates acridines, anthracyclines, and other classes of aromatic compounds, is the ability of porphyrins to generate ROS under the action of visible light and cause irreversible DNA damage.<sup>[7-9]</sup> To date, DNA complexes with tetrasubstituted cationic porphyrins have been the most studied. The asymmetry of the peripheral substituents of the porphyrin macrocycle can favourably affect the stability of the complexes formed with DNA and the selectivity of binding to GC or AT enriched DNA regions. Previously, we studied complexes of tricationic porphyrins containing benzimidazole (Npor), benzoxazole (Opor), and benzothiazole (Spor) residues with ssDNA.<sup>[10,11]</sup> Based on the spectral data of "fingerprints": the bathochromic shift of the Soret band and its hypochromism (> 40%), as well as the results of competitive titration with ethidium bromide, it was concluded that these porphyrins intercalated into DNA. In connection with new data on the nature of the interaction of ethidium bromide, that it is a multimodal ligand, *i.e.* can bind to DNA not only as an intracalate, but also in the major groove, it became necessary to clarify the nature of the Npor, Opor, and Spor complexes with nucleic acids. For these purposes, representative synthetic nucleic acids were selected containing exclusively G-C (poly[d(GC)2]) or A-T (poly[d(AT)2]) nitrogenous base pairs.

## Experimental

The studied porphyrins – 5-[4'-(1'',3''-benzothiazol-2''-yl)-phenyl]-10,15,20-tri-(N-methyl-3'-pyridyl)porphyrin triiodide (Spor), 5-[4'-(1'',3''-benzoxazol-2''-yl)phenyl]-10,15,20-tri-(N-methyl-3'-pyridyl)porphyrin triiodide (Opor) and 5-[4'-(N-methyl-1'',3''-benzimidazol-2''-yl)phenyl]-10,15,20-tri-(N-methyl-3'-pyridyl)porphyrin triiodide (Npor) were synthesised in the same way.<sup>[12]</sup>

Oligonucleotides poly[d(AT)2] and poly[d(GC)2] were synthesized by Synthol (Moscow, Russia). The concentrations of poly-

[d(AT)2], poly[d(GC)2] were determined spectrophotometrically using molar extinction coefficients:  $\epsilon(262 \text{ nm}) = 6600 \text{ cm}^{-1}\text{M}^{-1}$ ,  $\epsilon(254 \text{ nm}) = 8400 \text{ cm}^{-1}\text{M}^{-1}$  for poly[d(AT)2], and poly[d(GC)2], respectively. Thus, the DNA concentrations given in this work indicate the concentration of nitrogenous bases.

For preparing solutions a Tris-HCl buffer with pH 7.4 consisting 250 mL of 200 mM Tris with 400 mL of 100 mM HCl and 350 mL of type I water from water purification system, UP-2010 (ULAB, China) was used.

UV-Vis and fluorescence spectra were registered using an AvaSpec-2048 spectrophotometer (Avantes BV, Netherlands), with a temperature-controlled cell at 25 °C. The monochromatic LED VL425-5-15 (Roitner Lasertechnik GmbH., Germany) was used as excitation light sources for fluorescence study.

The time-resolved fluorescence measurements were carried out by means of a high-performance fluorescence lifetime and steady state spectrometer FluoTime 300 (PicoQuant, Germany) with a laser 450 nm impulse as an excitation source. The instrument response function (IRF) of the system was measured with the stray light signal of a dilute colloidal silica suspension (LUDOX®). The fluorescence decay curves were measured and the fluorescence lifetimes were obtained by reconvolution of the decay curves using the EasyTau 2 software package (PicoQuant, Germany).

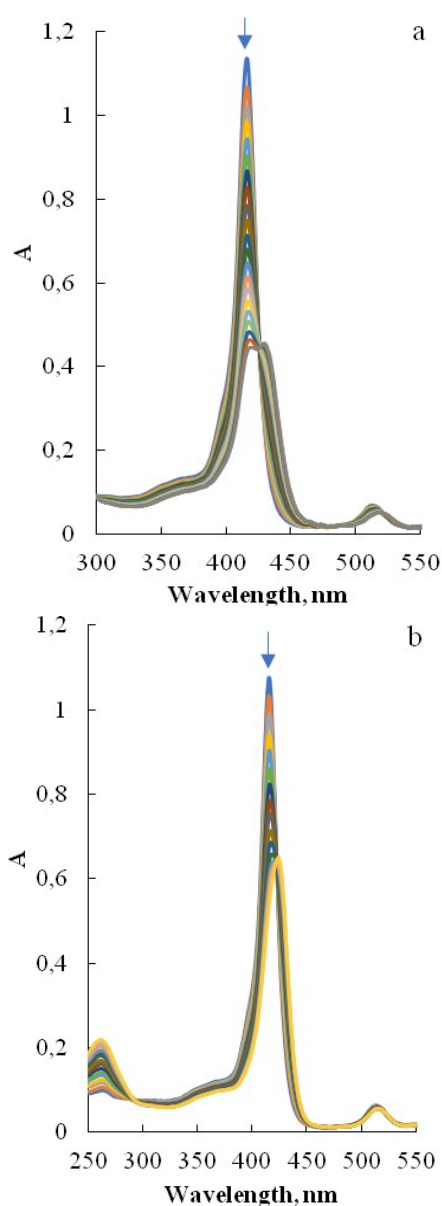
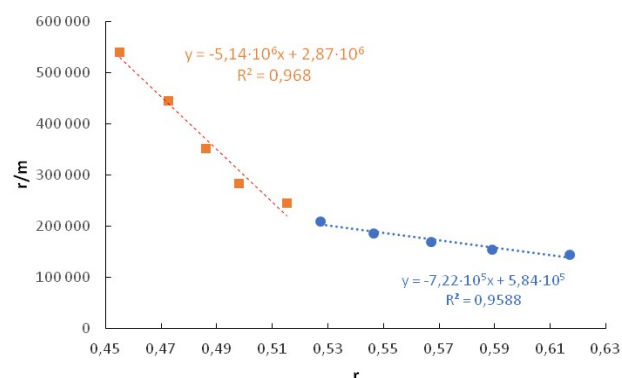
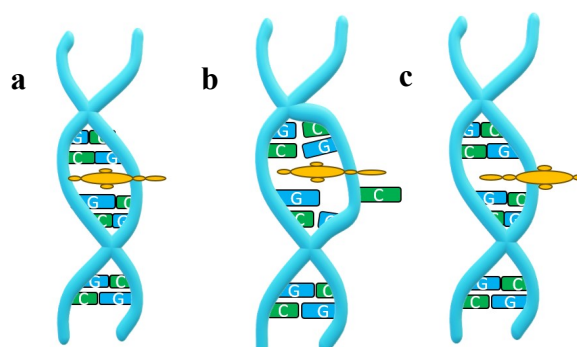
The affinity constants, R (DNA/Porphyrin Ratio) and a number of binding sites (n) were estimated according to Scatchard method<sup>[13]</sup> from spectral data.

## Results and Discussion

As an example, the absorption spectrum of Opor obtained by titration of poly[d(GC)2] (Figure 1a) and poly[d(AT)2] (Figure 1b) is presented. The appearance of the spectra of the porphyrins Spor and Npor upon titration with representative nucleic acids is similar, only the degree of hyperchromicity and the size of the bathochromic shift of the Soret band differ (Table 1). Analysing the data in Table 1, we can conclude that the complexation of the studied porphyrins with poly[d(AT)2] causes a smaller decrease in the intensity of the Soret band and its smaller bathochromic shift compared to the complexation of these porphyrins with poly[d(GC)2]. The resulting spectral changes reflect changes in the "fingerprint" region and indicate the formation of different types of complexes. In the case of complex formation of porphyrins with poly[d(AT)2], the recorded changes in the UV-Vis spectra of porphyrins indicate the formation of an external complexes, in which the porphyrin is located in the groove of the nucleic acid. The graphic dependence in Scatchard coordinates for the studied complexes of porphyrins with poly[d(AT)2] is linear, which indicates the formation of a complex of one type. The affinity constant of poly[d(AT)2] for porphyrins increases in the following order: Npor < Spor < Opor (1). The position of the porphyrin containing the benzimidazole residue is probably due to steric factors created by the N-CH3 group in the monoheteryl substituent of the porphyrin when Npor is introduced into the poly[d(AT)2] groove. The highest affinity of poly[d(AT)2] among the studied porphyrins poly[d(AT)2] exhibits to Opor, probably the higher electron-donating ability of the O atom compared to the S atom in Spor or the tertiary N atom in Npor allows additional stabilization of the Opor complex with poly[d(AT)2] due to H-bonding of the heteryl substituent Opor with deoxyribose poly[d(AT)2].

**Table 1.** Spectral changes of Soret band of porphyrin and Scatchard constant while complexation with nucleic acids.

System	Soret band hyperchromicity, %	Soret band bathochromic shift $\Delta\lambda$ , nm	Scatchard constant
Opor - poly[d(GC)2]	61	15	$2.64 \cdot 10^6$ $1.15 \cdot 10^7$
Spor - poly[d(GC)2]	63	15	$7.22 \cdot 10^5$ $5.14 \cdot 10^6$
Npor - poly[d(GC)2]	65	16	$3.34 \cdot 10^6$ $1.45 \cdot 10^7$
Opor - poly[d(AT)2]	40	9	$2.13 \cdot 10^7$
Spor - poly[d(AT)2]	42	12	$6.93 \cdot 10^6$
Npor - poly[d(AT)2]	45	12	$2.66 \cdot 10^6$

**Figure 1.** UV-Vis spectra of Opor ( $7.5 \cdot 10^{-6}$  M) during titration in TRIS with: (a) poly[d(GC)2] ( $0-2.25 \cdot 10^{-5}$  M); (b) poly[d(AT)2] ( $0-2.1 \cdot 10^{-5}$  M).**Figure 2.** Scatchard plot for the system Spor-poly[d(GC)2]. Titration was carried out by adding a solution of poly[d(GC)2] ( $0-2 \cdot 10^{-5}$  M) to a solution of Spor ( $8.6 \cdot 10^{-6}$  M) in TRIS at 25 °C.**Figure 3.** Schemes of possible intercalation complexes of DNA with porphyrins.

Spectral data obtained by titration of the studied porphyrins with poly[d(GC)2] correspond to the "fingerprints" of intercalation complexes. The graphical dependence in the Scatchard coordinates for the porphyrin-poly[d(GC)2] systems is not linear (Figure 2) and consists of two sections, which indicates the formation of complexes of 2 types.

Analysing the structure of porphyrin compounds and taking into account the intercalation nature of the interaction with poly[d(GC)2], we can assume the formation of complexes, schematically shown in Figure 3.

The formation of the complex shown in Figure 3a will be carried out due to the interaction of the  $\pi$ -system of the porphyrin macroring with the aromatic systems of nitrogenous bases. The studied porphyrins differ from each other only by the heteroatom in the monoheteryl substituent, which is rotated at an angle of about 20–30 degrees to the macrocycle, so the conjugation effect is unlikely. The inductive effect will also decay after 3–4 bonds; therefore, close values of the affinity constants for the intracalation complexes corresponding to the scheme in Figure 3a can be expected. Judging by the data obtained (Table 1), the affinity of these poly[d(GC)2] intercalation complexes with porphyrins lies within  $(2.6-5.14) \cdot 10^6$  and increases in the porphyrin series: Opor < Npor < Spor (2).

During the formation of the complex in Figure 3b, the  $\pi$ - $\pi$  interaction of the porphyrin macroring with nitro-

genous bases remains possible, but due to the distortion of one of the duplex helices, this interaction is incomplete. However, with this variant of complex formation, the possibility of additional interaction between the inverted nitrogenous base and the monoheteryl porphyrin substituent appears. Intercalation complexes corresponding to the scheme in Figure 3b are described in the literature for DNA systems with copper(II) *meso*-tetra(N-methyl-4-pyridyl)-porphyrin and  $[\text{Ru}(\text{bpy})_2\text{dppz}]^{2+}$  (where bpy = 2,2'-bipyridine and dppz = dipyrrophenazine).<sup>[14,15]</sup> The third type of complex (Figure 3c) is also known and described in the literature. In this case, the interaction between the aromatic system of the monoheteryl porphyrin substituent and nitrogenous bases occurs, and the macroheterocyclic ring is located in the groove of the nucleic acid. Hydrophobic interactions play an important role in the stabilization of the complex in Figure 3c. The affinity of poly[d(GC)2] in possible variants of intercalation complexes (Figure 3b or 3c) increases in the series of porphyrins: Spor < Opor < Npor (3). The numerical values of the affinity of poly[d(GC)2] for porphyrins and changes in the spectra during titration do not allow one to establish the type of the second complex formed, especially since the possibility of the formation of different types of complexes by different porphyrins is not excluded. For example, the van der Waals radius of the NCH<sub>3</sub> group is 3.5 Å, that of the sulfur atom is 1.85 Å, and that of oxygen is 1.4 Å. The interplanar distance of aromatic systems for the formation of a  $\pi$ - $\pi$ -bond should be 3.2–4.2 Å; accordingly, the NCH<sub>3</sub> group in the composition of Npor will sterically prevent the formation of the complex Figure 3c, and in the case of Spor and Opor, the formation of the complexes shown in Figure 3c is sterically admissible.

Valuable information about the fluorophore microenvironment can be obtained from the analysis of the fluorescence lifetime (Table 2). The pre-exponential factors (A<sub>i</sub>) reflect the percentage of fluorescent molecules with a fluorescence lifetime ( $\tau_i$ ) (Table 2).

The fluorescence decay rate of porphyrins in the studied solutions was measured for the Q(0.0) transition (in the range of 655–657 nm). As can be seen from the data in Table 2, upon excitation of individual porphyrins, there are two components in the Qx(0.0) band, one of which is short-lived, with a lifetime of about 1–2.6 ns. For cationic porphyrins, the appearance of a short-lived component is typical and, according to the data of this work,<sup>[16]</sup> is caused by intramolecular CT - charge (electron) transfer from

the porphyrin macrocycle after optical excitation to electron-deficient N-methylpyridyl groups. The energy of the ST state is almost equal to the energy of the excited singlet state of porphyrin S1. It is the mixing of the S1 and CT states, in which an electron is transferred from the porphyrin core to the electron-deficient pyridinium group, that explains the presence of the short-lived component. The studied porphyrins are characterized by relatively long fluorescence in aqueous media, since the average fluorescence lifetime of water-soluble porphyrins in an aqueous medium rarely exceeds 5 ns.<sup>[17]</sup> This makes the studied porphyrins promising candidates for bioimaging.

In the composition of solutions containing poly[d(AT)2], the fluorescence decay rate is described by a three-exponential dependence. When porphyrins are bound to poly[d(AT)2], the lifetime of the short-lived component and its fraction slightly decrease (Table 2). This indicates that the microenvironment in the region of N-methylpyridyl groups is changing. The mean-living component also decreases from (7.3–7.5 ns) in solutions of individual porphyrins to (4.2–6.1 ns) in solutions containing poly[d(AT)2]. It is likely that the decrease in the short-lived and medium-lived components of porphyrins is due to the orientation of macroheterocyclic compounds relative to the negatively charged backbone of poly[d(AT)2], and corresponds to the formation of an external weak electrostatic complex. In the interaction of porphyrins with poly[d(AT)2], as shown above, according to the data of electron spectroscopy, stable complexes with an external groove are formed. The fluorescence lifetime of porphyrins upon localization in the groove of the nucleic acid increases to (9.6–11.1 ns). This indicates a decrease in the nonradiative deactivation of the excited state of the porphyrin due to the isolation of the chromophore from the aqueous solvent, which is typical for porphyrin complexes localized in the major groove.<sup>[18-20]</sup>

In the composition of solutions containing poly[d(GC)2], the fluorescence decay rate is described by a biexponential dependence. The short-lived component disappears; there may be several reasons for this phenomenon. First, an additional interaction occurs between the N-methylpyridyl groups of the porphyrin and the negatively charged phosphate backbone of the nucleic acid, which are located in close proximity to each other in the intercalate (Figure 3a-c). Secondly, the  $\pi$ - $\pi$ -interaction of the macroring with nitrogenous bases will affect the energy of the excited singlet state of porphyrin S1. Both of these factors will negatively affect the mixing of the S1 and CT states.

**Table 2.** Fluorescence lifetime values of porphyrins and their complexes with nucleic acids in TRIS at 298 K ( $\lambda_{\text{ex}}=450$  nm).

System	Fluorescence life time, ns				Preexponential factor			$\chi^2$
	$\tau_1$	$\tau_2$	$\tau_3$	$\tau_{\text{av}}$	A1, %	A2, %	A3 %	
Opor	2.029	7.534		6.483	46.71	53.29		1.157
Spor	2.572	7.705		6.274	53.67	46.32		1.227
*Npor	1.312	7.317		5.664	32.06	67.94		1.154
Opor - poly[d(GC)2]	4.08	10.766		10.07	23.50	76.50		1.136
Spor - poly[d(GC)2]	3.466	9.245		6.774	66.59	33.41		1.170
*Npor - poly[d(GC)2]	4.54	11.171		10.573	19.7	80.3		1.126
Opor - poly[d(AT)2]	0.849	5.09	10.857	9.471	31.32	21.51	47.15	1.112
*Npor - poly[d(AT)2]	0.931	6.01	11.05	9.631	37.0	18.3	44.7	1.125
Spor - poly[d(AT)2]	0.835	4.19	9.55	6.702	48.06	31.10	20.84	1.1580

\*In press

As can be seen from the data obtained (Table 2), regardless of the nature of the heteroatom, the fluorescence lifetimes of porphyrins are close to each other within the framework of two components (3.5–4.54 ns) and (9.2–11.2 ns). The first component probably corresponds to the porphyrin in the composition of the intercalation complex shown in Figure 3a. The decrease in the porphyrin fluorescence lifetime upon binding to poly[d(GC)2] is apparently due to  $\pi$ - $\pi$  interaction with nitrogenous bases of the nucleic acid, which leads to an increase in nonradiative energy dissipation. It should be noted that for tetracationic porphyrins in the composition of intercalation complexes, the fluorescence lifetime is about 2 ns.<sup>[18,20]</sup> It is obvious that in the systems under study for the complexes shown in Figure 3a, a full-fledged  $\pi$ - $\pi$  interaction will be prevented by the distortion of one of the nucleic acid chains caused by the presence of a bulky monoheteryl substituent. It is noteworthy that the shorter Spor fluorescence lifetime in the composition of the Spor-poly[d(GC)2] complex (Table 2) corresponds to a higher affinity constant of the complex and its larger proportion of 66% (Table 1) compared to similar characteristics of the Opor and Npor complexes with poly[d(GC)2]. This indicates the dominant role of  $\pi$ - $\pi$  interactions between the porphyrin macrocycle and nitrogenous bases in the stabilization of the intercalation complex. As part of another type of intercalation complex (Figure 3b or 3c), the fluorescence lifetime of porphyrins increases significantly and, most surprisingly, it practically coincides with the lifetime of porphyrins in the complex with the outer groove poly[d(AT)2] (Table 2), but the affinity constants of poly[d(GC)2] and poly[d(AT)2] for porphyrins differ significantly (from 2 to 10 times, Table 1). The data obtained indicate a certain isolation of the chromophore in the poly[d(GC)2] intercalation complex from water molecules (fluorescence quencher). Unfortunately, both types of complexes fit this definition (Figure 3b,c), which does not allow us to determine the type of the resulting intercalation complex based on the data on the fluorescence decay rate.

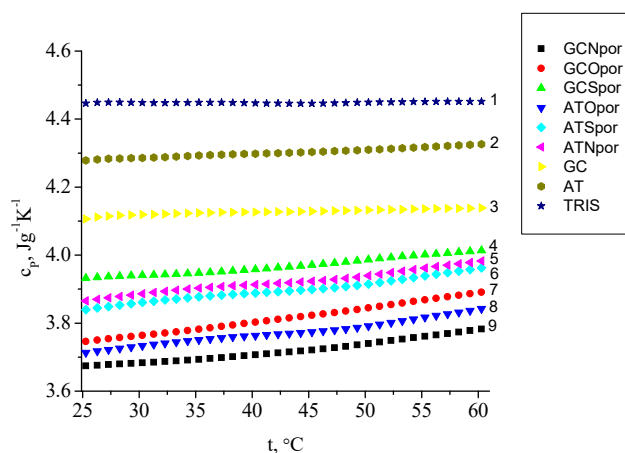


**Figure 4.** Temperature dependences of specific heat capacities of solutions: 1) TRIS; 2) poly[d(AT)2]-TRIS; 3) poly[d(GC)2]-TRIS; 4) poly[d(GC)2]-Spor-TRIS; 5) poly[d(AT)2]-Npor-TRIS; 6) poly[d(AT)2]-Spor-TRIS; 7) poly[d(GC)2]-Opor-TRIS; 8) poly[d(AT)2]-Opor-TRIS; 9) poly[d(GC)2]-Npor-TRIS.

Information about structural changes in solutions of nucleic acids (NA) upon interaction with porphyrins can be obtained by DSC by analysing the temperature dependences of heat capacities. To eliminate the effects of nucleic acid melting, the temperature range of 25–60 °C was analysed. Typical temperature dependences of the specific heat capacities of the studied solutions are shown in Figure 4.

For all nucleic acids, porphyrin binding also leads to a general decrease in the heat capacity of solutions, *i.e.* regardless of the type of complexes formed (intercalate or complex with a groove), *i.e.* the system stabilizes. For a correct analysis of the obtained data, correlation dependences of the specific heat capacity of solutions were constructed (Equation 1):

$$c_p(\text{NA-Por-TRIS}) = a + b \times \Delta c_p(\text{NA-Por}) + c \times c_p(\text{NA-TRIS}), \quad (1)$$

$$\text{where } \Delta c_p(\text{NA-Por}) = c_p(\text{NA-Por-TRIS}) - c_p(\text{TRIS})$$

The obtained coefficients *a*, *b* and *c* in equation (1) are presented in Table 3. The physical meaning of the coefficient is as follows: coefficient *b* - characterizes the proportion of structural changes in the analyzed solution associated with the interactions "NA-Por" occurring upon addition of the ligand.

The coefficient *c* characterizes such a proportion of structural changes in the NA-TRIS solution, which was preserved as a result of the interaction of the nucleic acid with the ligand. Accordingly, the coefficient (*1-c*) shows what proportion of the "NA-TRIS" bonds must be broken in order to realize the "NA-Por-TRIS" interaction.

The coefficient *a*, the free term of equation (1), shows the differences in the interaction energy of the solvent-solvent (TRIS-TRIS) and the solvent-solute "TRIS-NA" in close proximity to the complex (NA-Por-TRIS).

Consider the changes in the coefficients *a*, *b*, (*1-c*) (Table 3), two groups of complexes of porphyrins with nucleic acids are clearly visible with close values of all three coefficients.

The first group is the complexes of porphyrins with a groove in poly[d(AT)2], they correspond to smaller values of the coefficients *a*, *b* and (*1-c*). The sequence of increasing the parameters of the correlation ratios  $N_{por} < Spor < Opor$  coincides with the series of increasing affinity constants (1). Changes in the values of the coefficients *a* and (*1-c*) during the transition from *Npor* to *Opor* are more significant, while the coefficient *b* remains almost unchanged. This suggests that the solvent molecules in the immediate vicinity of the nucleotide undergo the greatest transformation during the formation of the complex with the groove. Indeed, the formation of a complex with a groove can lead to a slight contraction of the nucleotide helix, so the coefficient *b* changes little. The incorporation of porphyrin into the groove is accompanied by its complete or partial dehydration. Water that hydrates the nucleic acid is bound both through the direct formation of hydrogen bonds with hydrate-active centers, and through water bridges that form chains of highly ordered water molecules.<sup>[21]</sup> Highly ordered water molecules were found by X-ray diffraction analysis in the grooves of B-DNA<sup>[21,22]</sup> and received the name "hydrate ridge".<sup>[23,24]</sup> It is obvious that porphyrins incorporating into the groove of poly[d(AT)2] destroy the highly ordered structure of water,

and this occurs to the greatest extent in the case of Opor and to the least extent in the case of Npor. This sequence is consistent with the increase in size of the monoheteryl porphyrin substituent described above. Therefore, in the design of ligands that bind to DNA grooves, increasing the size of the monoheteryl substituent is impractical.

The second group of porphyrin-poly[d(GC)2] complexes is characterized by higher values of all three analyzed coefficients (Table 3). For all porphyrin-poly[d(GC)2] intercalation complexes, the coefficient *b* is greater than 1. This is due to the fact that there are significant structural changes in the analysed solution associated with the "NA-Por" interactions that occur when the porphyrin is added. During the intercalation of porphyrins, the helix is elongated due to its unwinding, and as shown above, due to the steric factors exerted by the monoheteryl substituent, one of the nucleic acid helices will be distorted during the formation of the complexes shown in Figure 3a,b. If the complex shown in Figure 3c is formed, then along with the above phenomena, the "hydrate ridge" will also be destroyed. The correlation parameters obtained for the porphyrin-poly[d(GC)2] systems are gross characteristics reflecting all the changes in the solution that occur during the formation of both types of intercalation complexes. Therefore, it is problematic to analyse their changes in the porphyrin series, since not only the type of the intercalation complex changes, but also its proportion. The highest values of the coefficients were obtained for the Npor-poly[d(GC)2] solution, which forms not the most stable intercalation complex according to the scheme of Figure 3a (Table 1) with a share of  $\approx 20\%$  (Table 2) and an intercalation complex corresponding to the scheme of Figure 3b with a share of  $\approx 80\%$  (Table 2). Slightly lower values of the coefficients *a*, *b* and (*I-c*) were obtained for the Spor-poly[d(GC)2] solution, for which the proportion of the classical intercalation complex is  $\approx 67\%$  (Table 2), and

the van der Waals atomic radius sulfur in the composition of the heteryl substituent makes the formation of a complex similar to Figure 3c unlikely. Thus, it can be assumed that in the Spor-poly[d(GC)2] system, the second intercalation complex corresponds to the scheme in Figure 3b and its share is about 33%.

## Conclusions

A spectral and thermochemical study of the processes of interaction of water-soluble monoheteryl-substituted porphyrins with poly[d(GC)2] and poly[d(AT)2] was carried out. It has been established that monoheteryl-substituted porphyrins containing residues of benzimidazole, benzoxazole, and benzothiazole molecules form complexes with the poly[d(AT)2] groove, destroying the "hydrate ridge" due to partial dehydration of the groove during porphyrin binding.

An increase in the size of the monoheteryl substituent negatively affects the stability of complexes with the nucleic acid groove. The complex formation of the studied porphyrins with poly[d(GC)2] leads to the formation of intercalation complexes of various types. In all cases, porphyrin intercalation results in distortion of one of the poly[d(GC)2] chains due to steric hindrance. The consequence of this is a weak  $\pi$ - $\pi$  interaction with the nitrogenous bases of the nucleic acid, isolation of the porphyrin fluorophore from water molecules, which leads to an abnormal increase in the fluorescence lifetime and can be used for bioimaging. The multicenter interaction found for porphyrin-poly[d(GC)2] systems, including intercalation with distortion of one of the nucleic acid strands, demonstrates a new potential opportunity to increase the selectivity of ligand binding to nucleic acids.

**Acknowledgements.** This work was supported by the Russian Science Foundation, grant no. 23-13-00235.

**Table 3.** Parameters of correlation relationships, coefficients *a*, *b* and *c* of Equation (1).

n		<i>a</i>	<i>b</i>	<i>c</i>	<i>I-c</i>	R	sd
1	Npor-poly[d(AT)2]-Tris	2.72±1.13	0.87±0.11	0.39±0.26	0.61	0.9984	0.001
2	Spor-poly[d(AT)2]-Tris	2.96±1.22	0.90±0.11	0.33±0.27	0.67	0.9985	0.001
3	Opor-poly[d(AT)2]-Tris	3.72±1.36	0.97±0.12	0.16±0.30	0.84	0.9986	0.001
4	Opor-poly[d(GC)2]-Tris	4.66±0.49	1.03±0.02	-0.05±0.12	1.05	0.9990	0.001
5	Spor-poly[d(GC)2]-Tris	4.76±0.39	1.06±0.03	-0.07±0.09	1.07	0.9972	0.001
6	Npor-poly[d(GC)2]-Tris	4.95±0.37	1.06±0.02	-0.11±0.09	1.11	0.9985	0.001
The sequence of changing the parameters of Equation (1)		increases (+)	increases (+)	decreases (-)			

## References

- Bray F., Jemal A., Grey N., Ferlay J., Forman D. *Lancet Oncol.* **2012**, *13*, 790. doi: 10.1016/S1470-2045(12)70211-5.
- Khattab M., Al-Karmalawy A.A. *Front. Chem.* **2021**, *9*, 628398. doi: 10.3389/fchem.2021.628398.
- Eldehna W.M., Abo-Ashour M.F., Nocentini A., Gratteri P., Eissa I.H., Fares M., Ismael O.E., Ghabbour H.A., Elaasser M.M., Abdel-Aziz H.A. *Eur. J. Med. Chem.* **2017**, *139*, 250. doi: 10.1016/j.ejmech.2017.07.073.
- Cheung-Ong K., Giaever G., Nislow C. *Chem. Biol.* **2013**, *20*, 648. doi: 10.1016/j.chembiol.2013.04.007.
- Bhaduri S., Ranjan N., Arya D.P. *Beilstein J. Org. Chem.* **2018**, *14*, 1051. doi: 10.3762/bjoc.14.93.
- Ferguson L.R., Denny W.A. *Mutat. Res.-Fund. Mol. M.* **2007**, *623*, 14. doi: 10.1016/j.mrfmmm.2007.03.014.
- Lebedeva N.S., Yurina E.S., Gubarev Y.A., Syrbu S.A. *Spectrochim. Acta, A* **2018**, *199*, 235. doi: 10.1016/j.saa.2018.03.066.
- Lebedeva N.S., Yurina E.S., Gubarev Y.A. *Spectrochim. Acta, A* **2019**, *215*, 153. doi: 10.1016/j.saa.2019.02.047.
- Koifman O.I., Ageeva T.A., Beletskaya I.P., Averin A.D., Yakushev A.A., Tomilova L.G., Dubinina T.V., Tsvivadze A.Yu., Gorbunova Yu.G., Martynov A.G., Konarev D.V.,

- Khasanov S.S., Lyubovskaya R.N., Lomova T.N., Korolev V.V., Zenkevich E.I., Blaudeck T., von Borczyskowski Ch., Zahn D.R.T., Mironov A.F., Bragina N.A., Ezhov A.V., Zhdanova K.A., Stuzhin P.A., Pakhomov G.L., Rusakova N.V., Semenishyn N.N., Smola S.S., Parfenyuk V.I., Vashurin A.S., Makarov S.V., Dereven'kov I.A., Mamardashvili N.Zh., Kurtikyan T.S., Martirosyan G.G., Burmistrov V.A., Aleksandriiskii V.V., Novikov I.V., Pritnov D.A., Grin M.A., Suvorov N.V., Tsigankov A.A., Fedorov A.Yu., Kuzmina N.S., Nyuchev A.V., Otvagin V.F., Kustov A.V., Belykh D.V., Berezin D.B., Solovieva A.B., Timashev P.S., Milaeva E.R., Gracheva Yu.A., Dodokhova M.A., Safronenko A.V., Shpakovsky D.B., Syrbu S.A., Gubarev Yu.A., Kiselev A.N., Koifman M.O., Lebedeva N.Sh., Yurina E.S. Macroheterocyclic Compounds – a Key Building Block in New Functional Materials and Molecular Devices, *Macroheterocycles* **2020**, *13*, 311–467. doi: 10.6060/mhc200814k.
10. Koifman O.I., Ageeva T.A., Kuzmina N.S., Otvagin V.F., Nyuchev A.V., Fedorov A.Yu., Belykh D.V., Lebedeva N.Sh., Yurina E.S., Syrbu S.A., Koifman M.O., Gubarev Y.A., Bunin D.A., Gorbunova Yu.G., Martynov A.G., Tsivadze A.Yu., Dudkin S.V., Lyubimov A.V., Maiorova L.A., Kishalova M.V., Petrova M.V., Sheinin V.B., Tyurin V.S., Zamilatskov I.A., Zenkevich E.I., Morshnev P.K., Berezin D.B., Drondel E.A., Kustov A.V., Pogorilyy V.A., Noev A.N., Eshtukova-Shcheglova E.A., Plotnikova E.A., Plyutinskaya A.D., Morozova N.B., Pankratov A.A., Grin M.A., Abramova O.B., Kozlovseva E.A., Drozhzhina V.V., Filonenko E.V., Kaprin A.D., Ryabova A.V., Pominova D.V., Romanishkin I.D., Makarov V.I., Loschenov V.B., Zhdanova K.A., Ivantsova A.V., Bortnevskaya Yu.S., Bragina N.A., Solovieva A.B., Kuryanova A.S., Timashev P.S. Synthesis Strategy of Tetrapyrrolic Photosensitizers for Their Practical Application in Photodynamic Therapy, *Macroheterocycles* **2022**, *15*, 207–302. doi: 10.6060/mhc224870k.
  11. Lebedeva N., Yurina E., Lebedev M., Kiselev A., Syrbu S., Gubarev Y. *Macroheterocycles* **2021**, *14*, 342. doi: mhc214031g.
  12. Gubarev Y.A., Lebedeva N.S., Yurina E.S., Syrbu S.A., Kiselev A.N., Lebedev M.A. *J. Pharm. Anal.* **2021**, *11*, 691–698. doi: 10.1016/j.jpha.2021.08.003.
  13. Peacocke A., Skerrett J.H. *Trans. Faraday Soc.* **1956**, *52*, 261. doi: 10.1039/TF9565200261.
  14. Lipscomb L.A., Zhou F.X., Presnell S.R., Woo R.J., Peek M.E., Plaskon R.R., Williams L.D. *Biochemistry* **1996**, *35*, 2818. doi: 10.1021/bi952443z.
  15. Song H., Kaiser J.T., Barton J.K. *Nat. Chem.* **2012**, *4*, 615. doi: 10.1038/nchem.1375.
  16. He X., Zhou Y., Wang L., Li T., Zhang M., Shen T. *Dyes Pigm.* **1998**, *39*, 173. doi: 10.1016/S0143-7208(98)00007-2.
  17. Kelly J.M., Murphy M.J., McConnell D.J., OhUigin C. *Nucleic Acids Res.* **1985**, *13*, 167. doi: 10.1093/nar/13.1.167.
  18. Chirvony V.S., Galievsky V.A., Kruk N.N., Dzhagarov B.M., Turpin P.-Y. *J. Photochem. Photobiol. B: Biol.* **1997**, *40*, 154. doi: 10.1016/S1011-1344(97)00043-2.
  19. Shen Y., Myslinski P., Treszczanowicz T., Liu Y., Koningstein J. *J. Phys. Chem.* **1992**, *96*, 7782. doi: 10.1021/j100198a052.
  20. Keane P.M., Kelly J.M. *Coord. Chem. Rev.* **2018**, *364*, 137. doi: 10.1016/j.ccr.2018.02.018.
  21. Maleev V., Semenov M., Kruglova E., Bolbuk T., Gasan A., Bereznyak E., Shestopalova A. *J. Mol. Struct.* **2003**, *645*, 145. doi: 10.1016/S0022-2860(02)00541-0.
  22. Drew H.R., Dickerson R.E. *J. Mol. Biol.* **1981**, *151*, 535. doi: 10.1016/0022-2836(81)90009-7.
  23. Banerjee D., Pal S.K. *J. Phys. Chem. B* **2007**, *111*, 10833. doi: 10.1021/jp074697n.
  24. Vega M.C., García Sáez I., Aymamí J., Eritja R., Van Der Marel G.A., van Boom J.H., Rich A., Coll M. *Eur. J. Biochem.* **1994**, *222*, 721. doi: 10.1111/j.1432-1033.1994.tb18917.x.

Received 10.07.2023

Accepted 19.09.2023